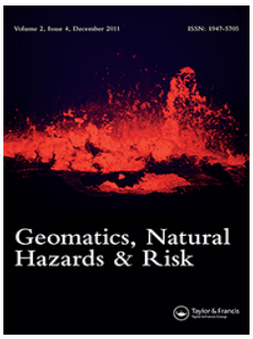

Geomatics, Natural Hazards and Risk

ISSN: 1947-5705 (Print) 1947-5713 (Online) Journal homepage: www.tandfonline.com/journals/tgnh20

Comparison and validation of per-pixel and object-based approaches for landslide susceptibility mapping

Thimmaiah Gudiyangada Nachappa, Stefan Kienberger, Sansar Raj Meena, Daniel Hölbling & Thomas Blaschke

To cite this article: Thimmaiah Gudiyangada Nachappa, Stefan Kienberger, Sansar Raj Meena, Daniel Hölbling & Thomas Blaschke (2020) Comparison and validation of per-pixel and object-based approaches for landslide susceptibility mapping, Geomatics, Natural Hazards and Risk, 11:1, 572-600, DOI: 10.1080/19475705.2020.1736190

To link to this article: https://doi.org/10.1080/19475705.2020.1736190

Published online: 28 Mar 2020.

GEOMATICS, NATURAL HAZARDS AND RISK
2020, VOL. 11, NO. 1, 572–600
https://doi.org/10.1080/19475705.2020.1736190

Comparison and validation of per-pixel and object-based approaches for landslide susceptibility mapping

Thimmaiah Gudiyangada Nachappa, Stefan Kienberger, Sansar Raj Meena, Daniel Hölbling and Thomas Blaschke

Department of Geoinformatics–Z_GIS, University of Salzburg, Salzburg, Austria

ABSTRACT

Remote sensing and geographic information systems (GIS) are widely used for landslide susceptibility mapping (LSM) to support planning authorities to plan, prepare and mitigate the consequences of future hazards. In this study, we compared the traditional per-pixel models of data-driven frequency ratio (FR) and expert-based multi-criteria assessment, i.e. analytical hierarchical process (AHP), with an object-based model that uses homogenous regions ('geon'). The geon approach allows for transforming continuous spatial information into discrete objects. We used ten landslide conditioning factors for the four models to produce landslide susceptibility maps: elevation, slope angle, slope aspect, rainfall, lithology, geology, land use, distance to roads, distance to drainage, and distance to faults. Existing national landslide inventory data were divided into training (70%) and validation data (30%). The spatial correlation between landslide locations and the conditioning factors were identified using GIS-based statistical models. Receiver operating characteristics (ROC) and the relative landslide density index (R-index) were used to validate the resulting susceptibility maps. The area under the curve (AUC) was used to obtain the following values from ROC for the per-pixel based FR approach (0.894) and the AHP (0.886) compared with the object-based geon FR approach (0.905) and the geon AHP (0.896). The object-based geon aggregation yielded a higher accuracy than both per-pixel based weightings (FR and AHP). We proved that the object-based geon approach creates meaningful regional units that are beneficial for regional planning and hazard mitigation.

ARTICLE HISTORY
Received 29 November 2019
Accepted 18 February 2020

KEYWORDS
Landslides; landslide susceptibility mapping; frequency ratio; analytical hierarchical process

1. Introduction

Natural disasters are significant adverse events resulting from the natural processes of the earth. These can be floods, landslides, hurricanes, tornadoes, volcanic eruptions, earthquakes or tsunamis (Tien Bui et al. 2019). Natural disasters have a severe impact on local economies and communities, and it can take several years to recover from the repercussions (Guzzetti et al. 2012). Natural disasters that affect the human

CONTACT Thomas Blaschke thomas.blaschke@sbg.ac.at

population have been occurring at an alarming rate around the globe in recent years. The leading cause of the disaster depends on the vulnerability of the region to the hazard. Landslides are one of the most frequently occurring natural hazards around the globe that cause economic losses, destruction of infrastructure and environmental problems (Li and Wang 2019). Landslides are instances of land degradation that change the topographies of the landscape, causing soil erosion and infrastructure damage (Pourghasemi and Rahmati 2018). In recent decades, landslides have received considerable attention from the scientific community and policymakers (Gordo et al. 2019). Europe has witnessed a significant number of fatalities and economic losses due to landslides, which occur as the result of a combination of meteorological, geological, morphological, physical and anthropogenic factors (Haque et al. 2016). To reduce the impact of landslides and losses, it is necessary to study the landslide susceptibility of a place (Meena et al. 2019a). Landslide susceptibility is defined as the probability of a landslide occurrence in a given area due to the effects of various conditioning factors (Hong et al. 2015). Landslide susceptibility mapping (LSM) is the crucial step in the landslide management of a region. Researchers have used different methods to analyze landslide susceptibility (Sestraș et al. 2019). LSM helps in effectively understanding the spatial distribution of probable landslide occurrences (Roodposhti et al. 2019).

The use of technologies like geographic information systems (GIS) and remote sensing can significantly help the responsible authorities in planning and mitigating the consequences of natural hazards. Remote sensing, along with GIS, has been one of the leading technologies for extracting and analyzing mass movements. In remote sensing and GIS, there are two main approaches for the classification and extraction of information from the images, namely per-pixel based and object-based and the per-pixel approach has been dominant, whereas object-based methods have become more widespread (Scaioni et al. 2014). Remote sensing using earth observation (EO) has been used for landslide susceptibility for inventory mapping, monitoring and rapid mapping (Casagli et al. 2016).

In this paper, the main aim is to compare per-pixel and object-based approaches for landslide susceptibility mapping and to gain insights about these two methodologies in regard to deriving susceptibility maps with higher accuracies for spatial planners and policymakers. We compare the traditional and straightforward per-pixel approaches of frequency ratio (FR) and a multi-criteria assessment approach building on analytical hierarchical process (AHP) weightings with an object-based aggregation method for landslide susceptibility analysis. For the per-pixel based approach, we selected FR as a data-driven model and the AHP multi-criteria assessment approach as an expert-based model. We used homogenous, spatial units – so-called geon - for the object-based analysis (Lang et al. 2014). The FR is a data-driven model based on the past landslide locations, causal factors and their spatial coverage (Wu et al. 2016). Many of the studies have used FR to generate susceptibility maps at regional scales, and there has been a strong correlation between the causal factors and the landslide locations in the area (Lee and Pradhan 2006). The AHP model based on expert knowledge in natural hazard susceptibility mapping is one of the most valued tools for susceptibility mapping (Feizizadeh and Blaschke 2014; Ghorbanzadeh et al. 2017;

Pirnazar et al. 2017). The geon concept was defined by Lang et al. (Lang et al. 2014), whereby geons are spatial units that are homogenous in terms of varying space-time phenomena under policy concern. Geons are specific types of regions, semi-automatically delineated with the incorporation of expert knowledge, scaled and of uniform response to an event under space-related policy concern. The initial methodology to model such 'integrated geon' was developed by Kienberger et al. (Kienberger et al. 2009). A main feature of the geon approach, is to identify homogenous regions without the restriction of administrative boundaries, thus reducing biases from the artificial borders such as administrative units (e.g. Modifiable Areal Unit Problem). There have been past studies assessing LSM for Austria where the focus has been on using only a few conditioning factors and an analysis based on statistical methods (Lima et al. 2017). There have also been studies explicitly focusing on lower Austria and assessing the quality of landslide susceptibility maps (Petschko et al. 2014). There are still challenges in landslide susceptibility mapping and the methods used (Glade et al. 2012). In a mountainous country like Austria, mass movements or landslides are a prevalent natural hazard, and mass movements often occur in areas that have been unstable in the past. The causes of mass movements are very diverse. The initiation of a mass movement can be influenced by several factors, such as precipitation, snowmelt, and earthquake vibration.

In this study, we compare simple yet widely used data-driven FR and expert-based AHP approaches for deriving the weights and introduce an object-based approach (geon) for identifying landslide susceptibility in Salzburg, Austria. Landslides constitute a significant hazard in Austria due to the alpine and mountainous areas. We used ten landslide conditioning factors, i.e. elevation, slope angle, slope aspect, rainfall, lithology, geology, land use, distance to roads, distance to drainage, and distance to faults, within four models to produce landslide susceptibility maps for Salzburg.

2. Study Area and Data

2.1. Study Area

Landslides are a prevalent natural hazard in the Province of Salzburg, Austria. Landslide occurrence in the study area is determined by several factors, namely lithology, tectonic structure, geomorphology (mainly slope angle and aspect) and land use. The geomorphological setting of Austria greatly contributes to the probability of landslide occurrence, as the Alps constitute 62% of the territory. Torrents and avalanches endanger around 75% of the communities in Austria (Höller 2009). The degradation of permafrost in the mountains due to the increase in temperatures can lead to slope instabilities and threatens settlements and transportations networks. In Austria, many human-made infrastructures, such as roads and buildings, are highly vulnerable to landslides caused by heavy rainstorms and long-lasting rain events.

The Province of Salzburg, the capital city of which is also called Salzburg, is one of the nine federal states in Austria (Figure 1). It has an area of 7,154.6 square kilometers and around 550,000 inhabitants. It stretches along its primary river, the Salzach, running from the central-eastern Alps in the south towards the north. The highest peak, the Großvenediger, reaches an altitude of 3657 meters above sea level.

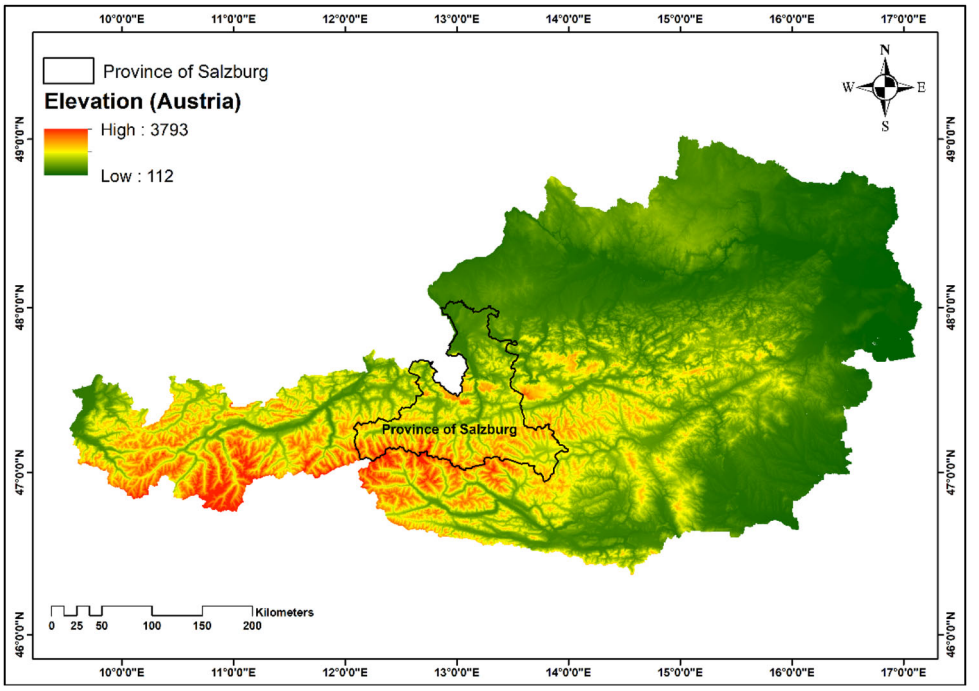

Figure 1. Location of the Province of Salzburg within the elevation map of Austria.

The province is covered by approximately 370,000 hectares of forest, corresponding to 52% of its total area. These forests have a high economic value and are essential for protection against natural hazards. This study area has been selected because no landslide susceptibility maps exist for it yet, and because it is prone to different types of landslides (e.g. rockfalls, shallow landslides, debris flows) causing damage to infrastructure and the loss of lives.

2.2. Landslide Inventory Data

The landslide inventory point dataset used for this study was obtained from the Geological Survey of Austria (GBA) (Figure 2). Despite the significant number of landslides occurring in Austria, only a limited number of landslide locations is included in the database. The available inventory data has limitations regarding completeness and up-to-datedness. For model validation, landslide inventory data which is not used for the analysis or training is required, which is why it is necessary to divide the dataset into two parts. The first part is applied to train the models and is called the training dataset, and the rest is used to verify the model's performance and is referred to as the validation dataset. There are no standard methodologies for the selection of training and validation samples (Guzzetti et al. 2012), but the most common ratio for training and validation samples is 70/30 (Tsangaratos and Ilia 2016). This approach has been used for various natural hazard studies (Umar et al. 2014). The landslide inventory dataset contained 560 landslide locations as of march 2019,

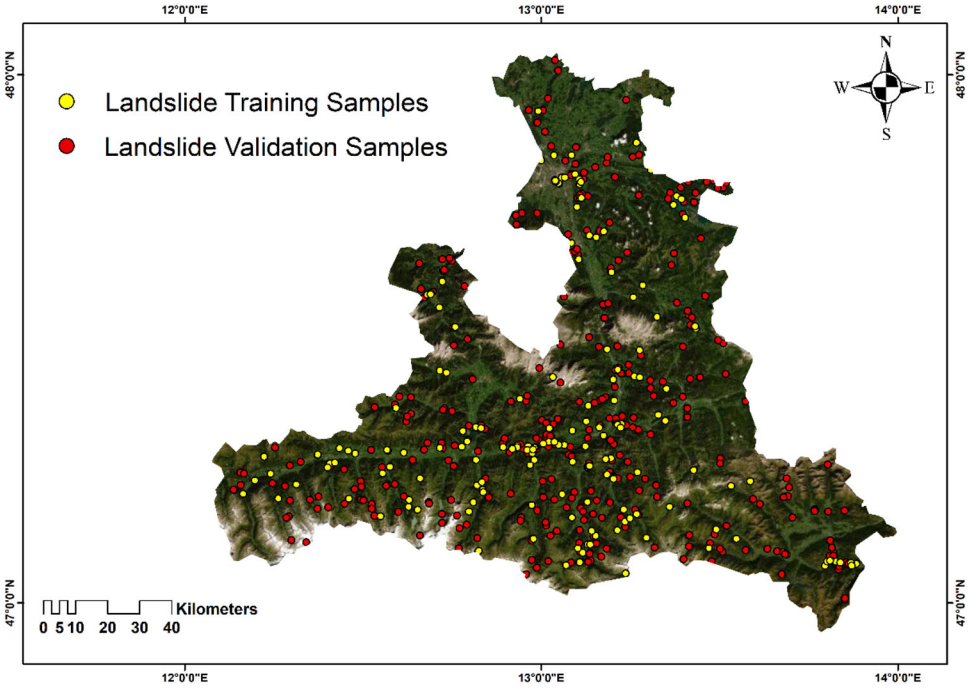

Figure 2. The GBA's landslide inventory locations classified into training and validation data for the Province of Salzburg.

and these were divided randomly into two groups, with 70% (392) used for training and 30% (168) used for validating the results.

2.3. Landslide Conditioning Factors

There are no predefined criteria for selecting the conditioning factors for the landslide susceptibility mapping. Ideally, the selected conditioning factors are operative, quantifiable and non-uniform. Based on the geomorphological characteristics, literature and on expert feedback, ten landslide conditioning factors were selected for this study area. The ten landslide conditioning factors selected were, namely elevation, slope angle, slope aspect, distance to roads, distance to drainage, precipitation, land use, faults, geology, and lithology. A freely available digital elevation model (DEM) with 10 m spatial resolution of the federal state of Salzburg, downloaded from the Open Data Portal Austria (www.data.gv.at), was used to derive slope and aspect layers. The land use map was downloaded from the Land Information System Austria (LISA). The lithology, geology and fault data were obtained from the Geological Survey of Austria. The drainage and road networks were downloaded from the humanitarian open street map network (HOTOSM). Rainfall data was downloaded from ÖKS15 from the data center of the Climate Change Centre Austria (CCCA). All the data were processed and used to generate the landslide conditioning factors in ArcGIS software. See Figure 3 for all the input conditioning factors.

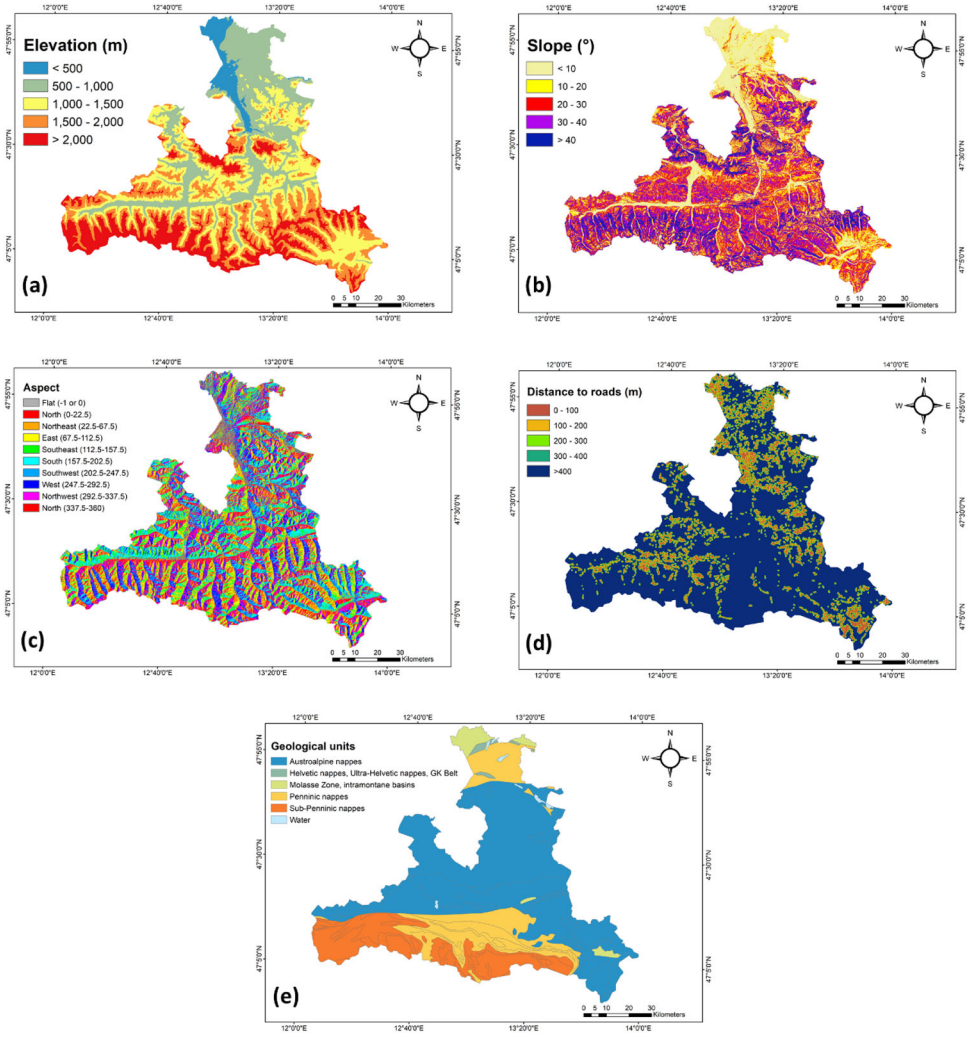

Figure 3. Map of the conditioning factors used in this study: (a) elevation, (b) slope, (c) aspect, (d) distance to roads, (e) geology, (f) lithology, (g) landuse, (h) distance to drainage, (i) distance to faults, (j) rainfall

The slope is one of the most critical factors contributing to slope failure (Pham et al. 2018). Slope is directly linked to landslides and topographies with steeper slopes are usually more susceptible to failure. The slope angle was derived from the DEM and classified into five classes from 0° to >40° with intervals of 10°.

The aspect is also an essential factor for landslide susceptibility analysis (Ghorbanzadeh et al. 2018b). Aspect describes the direction of the slope. We classified the slope aspect into ten classes: north (0°–22.5°; 337.5°–360°), northeast (22.5°–67.5°), east (67.5°–112.5°), southeast (112.5°–157.5°), south (157.5°–202.5°), southwest (202.5°–247.5°), west (247.5°–292.5°), northwest (292.5°–337.5°), north (337.5°–360°) and flat (0°).

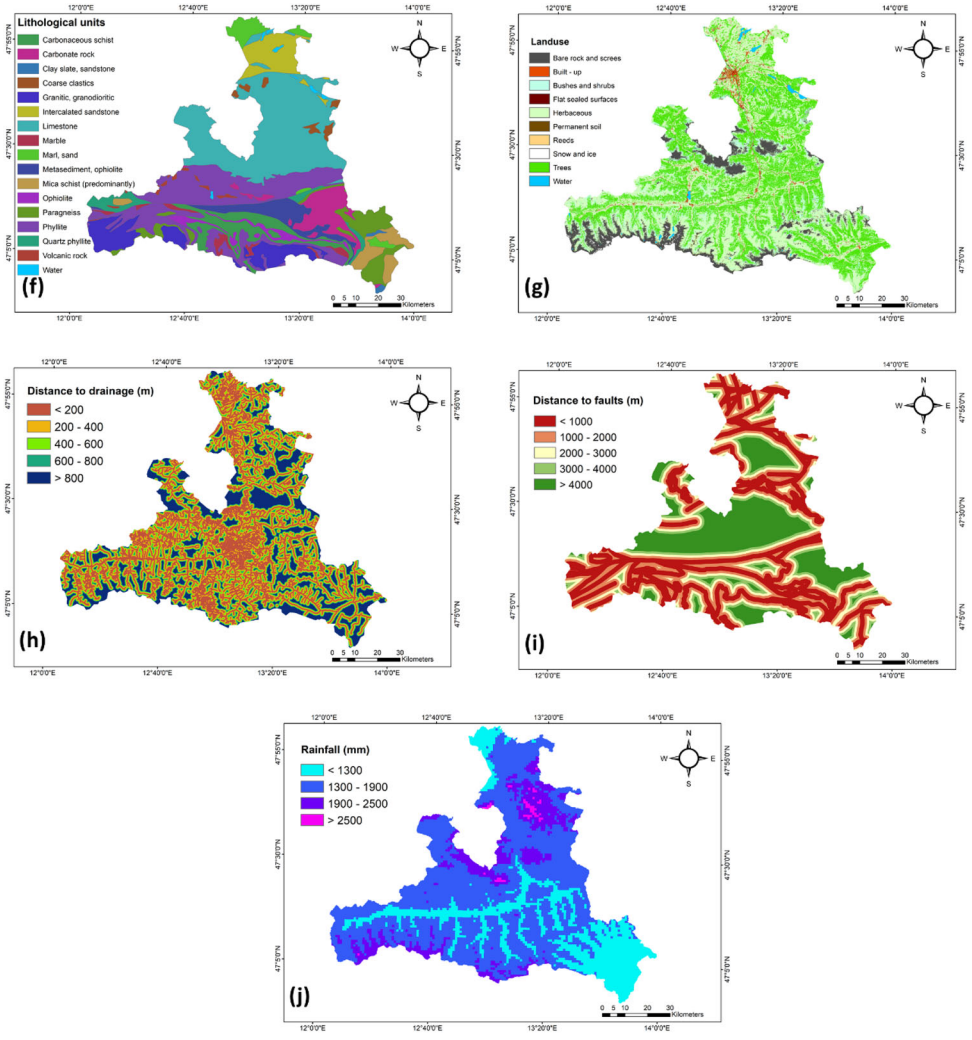

Figure 3. Continued.

The elevation influences the geomorphological and geological processes (Raja et al. 2017). It can affect the topographic attributes that lead to spatial variability of different landscape processes, and it can influence the vegetation distribution. Elevation was classified into five classes: 0–500 m, 500–1000 m, 1000–1500 m, 1500–2000 m and >2000 m above mean sea level.

Drainage is another important factor for landslide analysis as it delivers water that causes material saturation, resulting in landslides in the valleys (Lee and Pradhan 2006). The study area was classified into five classes reflecting the distance to drainage, namely 0–250 m, 250–500 m, 500–750 m, 750–1000 m and >1000 m.

The distance to roads is a further causal factor for landslide occurrence (Meena et al. 2019a). Roads are regarded as one of the most critical anthropogenic factors influencing the occurrence of landslides. The study area was classified into five different classes, which designated the influence of roads on landslide occurrence. The

buffer zone intervals were defined as 0–100 m, 100–200 m, 200–300 m, 300–400 m and >400 m. We chose these intervals as most of the landslides caused by road construction occur within 500 m of the road network.

Lithology is widely accepted as one of the most important factors in landslide susceptibility studies (Chen et al. 2017). Lithological units vary in terms of geological strength indices, susceptibility to failure and permeability (Yalcin and Bulut 2006). The variation of lithological units may lead to a variation in the strength and permeability of the rock stratum. Usually, the mass movements slide along a rock stratum with low strength and poor permeability. We have seventeen lithological units in our study area.

Geology is also one of the essential factors in landslide studies (Chen et al. 2017). We have six geological units in our study area such as austroalpine napes, Helvetic nappes, molasses zones, penninnic nappes, sub-penninic nappes and water.

Land use is another landslide-related factor in landslide susceptibility mapping, and it has been widely applied in previous research (Bartelletti et al. 2017; Persichillo et al. 2017). Variation in land use can explain the highly dissected zones within the region and provide insight into the landslide activity that is likely to occur. Land use and land cover data was downloaded from LISA and was classified into ten classes: built-up, flat sealed surfaces, permanent soil, bare rock and screes, water, snow and ice, trees, bushes and shrubs, herbaceous, and reeds.

Distance to faults is another factor determining the occurrence of landslides. Faults create a gap between two distinctive lithological units and generate fractures and joints within the lithological unit that can propagate landslide activity. Geological faults are responsible for triggering a large number of landslides because the tectonic breaks usually decrease the surrounding rock strength. The faults were derived from the geology layer obtained from the GBA. The distance to faults factor was classified into intervals of 0–1000 m, 1000–2000 m, 2000–3000 m, 3000–4000 m and >4000 m.

Rainfall is often considered as the main triggering factor for landslide initiation and also a key factor for landslide susceptibility analysis (Wu et al. 2016). Rainfall characteristics vary by weather conditions and topographical characteristics, causing considerable temporal and spatial differences in rainfall amount and intensity, which can trigger landslides both over large areas but also only in specific small areas. Annual precipitation data were obtained from ÖKS15 as annual average precipitation for Salzburg province and was classified into the following four classes: 0-1300 mm, 1300-1900 mm, 1900-2500 mm and >2500 mm.

3. Methods

The Landslide susceptibility analysis was carried out using two traditional weighting approaches commonly used in per-pixel models, namely the data-driven FR and multi-criteria assessment expert-based AHP. There are various approaches for landslide susceptibility mapping and the main reason for choosing the data-driven and expert-based approach for weighting was to understand the impact of aggregation using object-based geons on simple, established yet widely used approaches. We used geons, which is an object-based aggregation approach, where the weights are derived

from data-driven FR, and expert-based AHP approaches for aggregation and to produce landslide susceptibility maps.

3.1. Weighting Approaches

3.1.1. Frequency Ratio (FR)

The FR model is widely used in landslide susceptibility analysis. FR is a simple assessment tool that gives the probability of the distribution of occurrence and non-occurrence of landslides for each conditioning factor (Lee and Pradhan 2006; Wang and Li 2017). The FR is a variation of the probabilistic model and is based on the observed relationships between the distribution of landslides and the related factors of each landslide (Tay et al. 2014). Thus, the FR shows the correlation between landslide locations and the conditioning factors influencing the occurrence of landslides in the given area. Landslide conditioning factors can be weighted by considering the ratio of observed landslides to the area of the given study area. Correlation between factor classes can be found through FR, which is quite a useful geospatial assessment tool (Mahalingam et al. 2016; Meena et al. 2019b). FR weights can be computed using the ratios of landslide inventory points of all classes within each factor. The landslide inventory points are then overlaid with the conditioning factors to obtain the area ratio for each factor class to the total area. The FR weights are then obtained by dividing the landslide occurrence ratio in a class by the area in that class (Demir et al. 2012).

3.1.2. Analytical Hierarchical Process (AHP)

The multi-criteria assessment based AHP is a decision-making tool to deal with complex, unstructured and multi-attribute problems, and was first developed by Saaty (Saaty 1980). The AHP model has been widely applied in various fields, including landslide susceptibility analysis (Kayastha et al. 2013). The AHP model is based on multi-criteria and involves the participation of experts and their expert knowledge and judgement (Saaty and Vargas 1984). Based on the importance of each factor, a hierarchical order of factors and numerical values are established (Cabrera-Barona and Ghorbanzadeh 2018; Ghorbanzadeh et al. 2018c). These factors are then integrated, and each factor is weighted according to its importance (Sahnoun et al. 2011). The AHP model is used for creating the correlative pairwise comparison matrix, which is generated from the expert's values based on their knowledge by comparing the importance of each factor to all the other factors. Each layer is assigned values based on the nine-point scale and added to the matrix. An underlying scale is proposed for pairwise comparisons in the AHP model, with values ranging from 1 to 9 (Table 1) (Saaty and Vargas 1991).

The expert assigns a value for each factor. The principle of transitivity is important in AHP for any given three factors (such as f1, f2 and f3), and is defined as follows; if f1 $>$ f2 and f2 $>$ f3, then f1 $>$ f3. The principle of transitivity is a basis for conditioning factor weighing in AHP. Due to this principle, a consistent pairwise comparison matrix would require that if 2f1 $>$ f2 (i.e., f1 is two times more preferable than f2) and 4f2 $>$ f3, then 8f1 $>$ f3 to account for the transitivity principle

Table 1. Pairwise comparison point-based rating scale of AHP

Importance Level	Ranking
Equally important	1
Equally important to slightly more important	2
Slightly more important	3
Slightly more important to much more important	4
Much more important	5
Much more important to very much more important	6
Very much more important	7
Very much more important to extremely important	8
Extremely important	9

(Ghorbanzadeh et al. 2017; Taha et al. 2019). Inconsistency can be defined based on the observation that $\lambda max > n$ for comparison matrices and$\lambda max > n$, if C is a consistent comparison. The consistency ratio (CR) is defined by Equation (1):

$$CR = (\lambda max - n)/(RI(n-1)) \tag{1}$$

where RI is the random index of a randomly created pairwise comparison matrix for n = 2, 3, 4, 5, 6, 7, 8, and 9. If the consistency ratio is <0.10, it indicates an acceptable level of consistency, whereas a CR > 0.10 points to a degree of inconsistency (Saaty and Vargas 1984). Surveys were conducted to gather expert knowledge from the Province of Salzburg to calculate the criteria weights using the AHP model. We chose professionals with expertise in the field of geology, landslides, geography, ecology and geoinformatics to fill in the questionnaire.

3.2. Aggregation Approaches

3.2.1. Per-pixel based aggregation

Spatial decision problems have given rise to multi-criteria decision analysis (MCDA). MCDA provides an assortment of techniques and procedures for organizing decision problems and designing decisions evaluation criteria (Malczewski 2006). There are two important multi-criteria evaluation methods in GIS: the Boolean overlay operations and weighted linear combinations, which are the most widespread within the ordered weighted average (Malczewski 1999).

In this study, we use the per-pixel based data-driven FR, and the expert-based AHP approaches to aggregate the weights. The FR approach uses the weighted sum approach, whereas the AHP uses the weighted overlay approach to produce the final susceptibility map.

The landslide susceptibility index (LSI) was calculated by the summation of each conditioning factor ratio value derived from the FR approach using the equation given below (Lee and Pradhan 2006). Equation (2):

$$\begin{aligned} LSI &= \sum FR \\ LSI &= (slope * w) + (aspect * w) + (elevation * w) + (distance\ to\ faults * w) \\ &\quad + (distance\ to\ road * w) + (distance\ to\ drainage * w) + (landuse * w) \\ &\quad + (lithology * w) + (geology * w) + (rainfall * w) \end{aligned} \tag{2}$$

Where LSI is the landslide susceptibility index, and FR is the frequency ratio of each factor type or class and w is the weight of each conditioning factor. In the relationship analysis, an FR value of 1 means that the class has a density of landslides proportional to the size of the class on the map; therefore, a value of 1 is an average value. LSI values greater than 1 signify a higher correlation, whereas values of less than 1 mean a lower correlation. The greater the LSI value, the higher the susceptibility to landslide occurrence. In contrast, the lower the LSI value, the lower the susceptibility to landslide occurrence.

The assessed weights of the ten layers were calculated using the AHP model based on the resulting pairwise comparison matrices. The AHP weights are aggregated based on a pairwise comparison matrix using the weighted overlay method to derive the final susceptibility map.

3.2.2. Object-based aggregation

3.2.2.1. *Geon*. Geons are defined rather broadly as spatial units that are homogenous in terms of varying space-time phenomena under policy concern, and the term itself is defined by Lang et al. (Lang et al. 2014) as "geon (derived from Greek gē (Γῆ) = land, earth and the suffix -on = something being) is a type of region, semi-automatically delineated with expert knowledge incorporated, scaled and of uniform response to a phenomenon under space-related policy concern". A geon is a scale-specific spatial object with stability features such as minimized inner variance and gradients towards the outside through vector encoding (Hagenlocher et al. 2014; Lang et al. 2014). The geon approach works in a two-step process to accomplish domain-specific (i.e., expert-based) and semi-automated regionalisation. In general, the geon approach, which generates composite objects (Tiede et al. 2010), is applied to multispectral data in an analytical, taxonomic process followed by an advanced mapping scheme (Lang et al. 2014). A specific type of multicomponent regionalisation is the region-based image segmentation, where results are generated based on spatial continuity and specific homogeneity criteria.

Multi-resolution segmentation is a widely used algorithm in object-based image analysis (OBIA) (Blaschke 2010). It generates homogenous image segments in a nested hierarchy of scaled representations. Spectral information is aggregated in a scale-adaptive manner, while the loss of detail is minimized (Dragut et al. 2014). The aim of generating geon is to map policy-relevant spatial phenomena in an adaptive and expert-validated manner, comparable to the respective scale of intervention. This helps to visualize and comprehend the spatial distribution of such phenomena and thereby to better plan, locate and evaluate intervention measures (Kienberger et al. 2009).

All segmentation processes and parameterisations were carried out in eCognition software. Before the segmentation process, all the conditioning factor layers were converted to 8 bit with normalized values from 0-255 and in GeoTIFF format for geon computation in eCognition. The normalization was calculated based on Equation (3):

$$V' = \frac{V - Vmin}{Vmax - Vmin} * 255 \tag{3}$$

Where V′ is the normalized value, V the causal factor value to be normalized, Vmin the minimum value of the whole data range and Vmax the maximum value of the data range for the particular layer. The most common algorithm in OBIA for segmenting an

image into image objects is the multi-resolution segmentation (MRS) (Baatz and Schäpe 2000). MRS starts at the pixel level and successively aggregates the pixels into objects of different shapes, sizes, and characteristics until it reaches a threshold of homogeneity set by the user. One of the main issues in MRS is the selection of parameters, especially the scale parameter (SP). The Estimation of Scale Parameter tool (ESP) allows detecting optimal scales based on a local variance graph, using a single layer (Drăguţ et al. 2010). This approach was extended into an automated tool (ESP2) for multiple layers (Dragut et al. 2014). The ESP2 tool is an entirely automated method for the selection of scale parameters that delivers three distinct scales using MRS, implemented in the eCognition Developer software. We used the ESP2 tool to get the optimal scale values, and the finest scale was used for generating the geon.

The aggregation based on the object-based geon approach was based on the weights from both the data-driven FR approach and the expert-based AHP approach. This enables us to compare the per-pixel approach against the object-based approach.

4. Results

4.1. Per-pixel

Landslide susceptibility maps were generated to identify the areas that are susceptible to landslides. The weights for the FR were derived from the data, and the AHP approach was based on the pairwise comparison matrix generated by the experts. The final weights for FR and AHP for each conditioning factor are given in Table 2. The weights for the FR were calculated in excel using the formula in ArcGIS software, and the AHP was calculated based on the expert's weights using Matlab software. The values for the LSM maps were in the range of 0 to 100.

The weights for each class of the conditioning factors for FR and AHP are given in Table 3. These weights were used to derive the final weights for each of the conditioning factors, which were used to create the final landslide susceptibility map.

There is no standard method for classifying the values in the resulting susceptibility maps. All the results were normalized to values between 0 and 100 for consistency and comparison. The results were classified into the five classes for 'very low', 'low', 'moderate', 'high' and 'very high' susceptibility classes using the quantile classification method, which distributes the values into groups that contain an equal number of

Table 2. Per-pixel based normalized weights for each factor from the data-driven FR and expert-based AHP approaches.

Factors	FR weights	AHP weights
DEM	5.26	5
Slope	3.04	18
Aspect	1.37	5
Distance to roads	1.82	5
Rainfall	5.19	15
Distance to drainage	4.44	8
Lithology	1.96	12
Geology	5.24	12
Distance to faults	1	8
Landcover	4.4	12

Table 3. Normalized weights for each factor and each of the classes based on the FR and AHP model.

Factors weights	Classes	Pixels per Class	% of Pixels	Landslide Pixels	% of Landslide Pixels	FR weights	AHP weights	Consistency Ratio (CR)
Distance to roads (m)	0–100	5339732	7.46	2500	6.38	0.86	0.41	0.003
	100–200	5304115	7.41	3300	8.42	1.14	0.23	
	200–300	4991679	6.97	3900	9.95	1.43	0.12	
	300–400	4595739	6.42	3600	9.18	1.43	0.12	
	>400	51359740	71.74	25900	66.07	0.92	0.12	
Distance to drainage (m)	<250	24233421	33.85	19400	49.49	1.46	0.40	0.007
	250-500	16105418	22.50	9100	23.21	1.03	0.24	
	500-750	11083956	15.48	4700	11.99	0.77	0.14	
	750-1000	7381373	10.31	3400	8.67	0.84	0.14	
	>1000	12786837	17.86	2600	6.63	0.37	0.08	
Distance to faults (m)	0–1000	23931781	33.43	14800	37.76	1.13	0.36	0.016
	1000–2000	14544140	20.32	7900	20.15	0.99	0.22	
	2000–3000	9329060	13.03	5000	12.76	0.98	0.22	
	3000–4000	6411517	8.96	3300	8.42	0.94	0.12	
	>4000	17374507	24.27	8200	20.92	0.86	0.08	
Slope (°)	0–10	13754900	19.23	4700	11.99	0.62	0.10	0.002
	20-30	13544556	18.94	7200	18.37	0.97	0.18	
	20-30	18498297	25.87	9900	25.26	0.98	0.18	
	30-40	16739088	23.41	10100	25.77	1.10	0.18	
	>40	8977191	12.55	7300	18.62	1.48	0.35	
Elevation (m)	0–500	3119650	4.36	1400	3.57	0.82	0.17	0.020
	500–1000	16946654	23.68	17300	44.13	1.86	0.39	
	1000–1500	21365633	29.85	11800	30.10	1.01	0.23	
	1500–2000	17868155	24.96	4800	12.24	0.49	0.11	
	>2000	12279629	17.16	3900	9.95	0.58	0.11	
Aspect	Flat	8437454	11.80	3200	8.16	0.69	0.06	0.011
	North	8549903	11.96	3800	9.69	0.81	0.06	
	Northeast	7994468	11.18	4800	12.24	1.10	0.12	
	East	7337976	10.26	4400	11.22	1.09	0.11	
	Southeast	7156275	10.01	5400	13.78	1.38	0.21	
	South	7022701	9.82	4800	12.24	1.25	0.20	
	Southwest	7985544	11.17	4800	12.24	1.10	0.12	
	West	8374074	11.71	4400	11.22	0.96	0.07	
	Northwest	8655637	12.10	3600	9.18	0.76	0.05	

(*continued*)

Table 3. Continued.

Factors weights	Classes	Pixels per Class	% of Pixels	Landslide Pixels	% of Landslide Pixels	FR weights	AHP weights	Consistency Ratio (CR)
Landuse	Built - up	773257	1.08	200	0.51	0.47	0.04	0.015
	Flat sealed surfaces	550481	0.77	600	1.53	1.99	0.21	
	Permanent soil	441228	0.62	100	0.26	0.41	0.04	
	Bare rock and screes	6501809	9.09	2500	6.39	0.70	0.08	
	Water	523557	0.73	0	0.00	0.00	0.03	
	Snow and ice	174977	0.24	200	0.51	2.09	0.23	
	Trees	26758131	37.41	15000	38.36	1.03	0.10	
	Bushes and shrubs	7783076	10.88	3700	9.46	0.87	0.09	
	Herbaceous	28013037	39.17	16800	42.97	1.10	0.14	
	Reeds	5672	0.01	0	0.00	0.00	0.03	
Lithology	Water	338887	0.47	0	0.00	0.00	0.01	0.010
	Limestone	20114817	28.13	9400	23.98	0.85	0.05	
	Coarse clastics, marl, shale, sandstone	764607	1.07	600	1.53	1.43	0.09	
	Intercalated sandstone and marlstone	3754579	5.25	1400	3.57	0.68	0.04	
	Phyllite	14754212	20.63	12400	31.63	1.53	0.10	
	Carbonate rock	4092521	5.72	1200	3.06	0.53	0.03	
	Quartz phyllite	1735326	2.43	600	1.53	0.63	0.03	
	Volcanic rock	385675	0.54	100	0.26	0.47	0.03	
	Marl, sand, gravel, limestone	1990847	2.78	300	0.77	0.27	0.02	
	Mica schist (predominantly)	2447252	3.42	1700	4.34	1.27	0.09	
	Marble	1156336	1.62	300	0.77	0.47	0.03	
	Metasediment, ophiolite	3551132	4.97	2500	6.38	1.28	0.09	
	Paragneiss	4234756	5.92	2000	5.10	0.86	0.05	
	Ophiolite	1490701	2.08	1300	3.32	1.59	0.12	
	Clay slate, sandstone, conglomerate	221302	0.31	200	0.51	1.65	0.13	
	Granitic, granodioritic, tonalitic gneiss	5603384	7.84	2600	6.63	0.85	0.05	
	Schist, quartzite, ophiolite	4875629	6.82	2600	6.63	0.97	0.05	
Geology	Water	338887	0.47	0	0.00	0.00	0.32	0.089
	Helvetic nappes, Ultra-Helvetic nappes	409412	0.57	300	0.77	1.34	0.21	
	Austroalpine nappes	42091508	58.86	23900	60.97	1.04	0.14	
	Penninic nappes	13672041	19.12	7800	19.90	1.04	0.14	
	Molasse Zone, intramontane basins	1990847	2.78	300	0.77	0.27	0.06	
	Sub-Penninic nappes	13009268	18.19	6900	17.60	0.97	0.13	
Rainfall (mm)	<1300	17539500	24.50	15900	40.66	1.66	0.42	0.004
	1300-1900	44101200	61.61	20300	51.92	0.84	0.23	
	1900-2500	9417200	13.16	2600	6.65	0.51	0.12	
	>2500	523900	0.73	300	0.77	1.05	0.23	

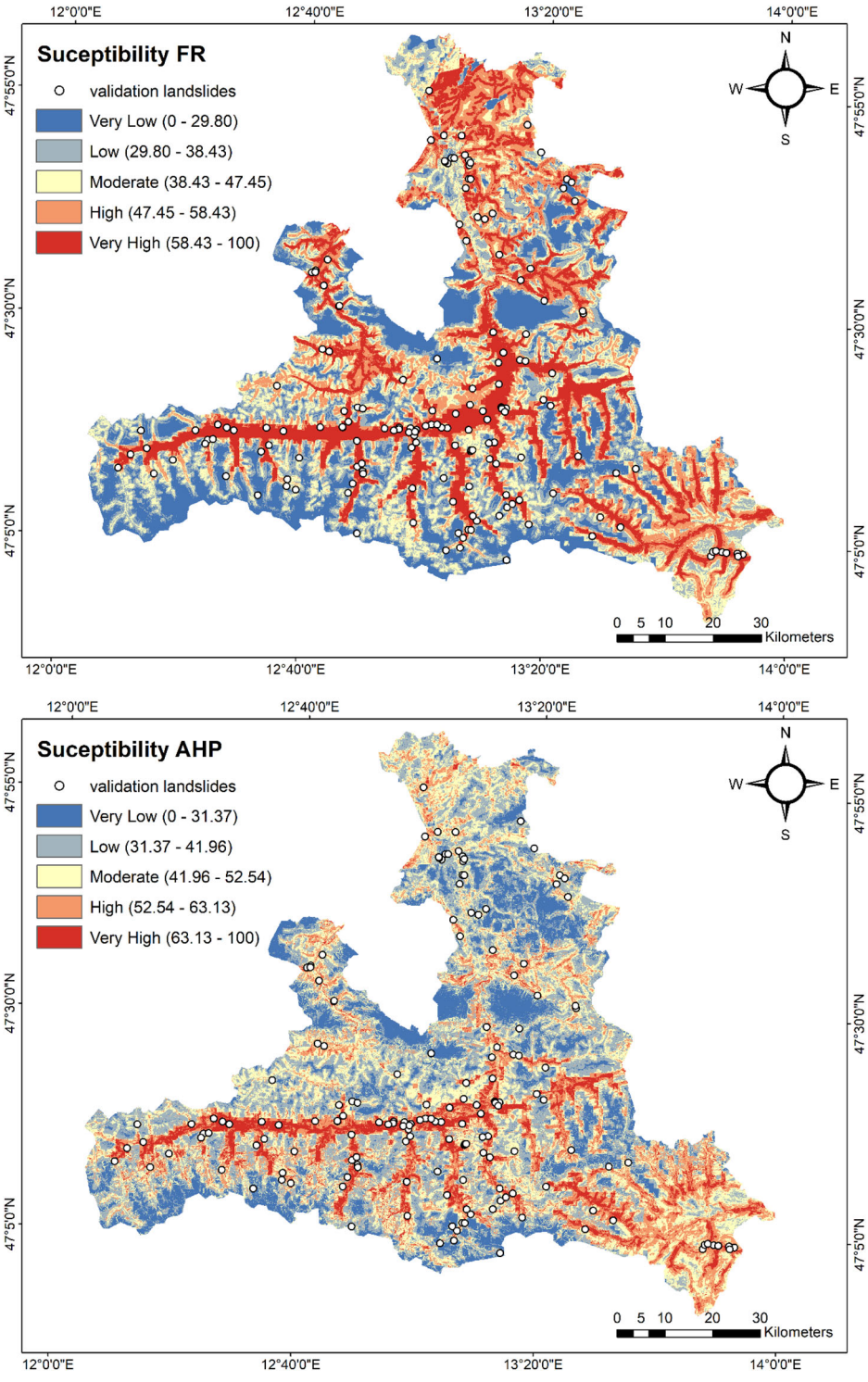

Figure 4. Landslide susceptibility maps derived using the per-pixel weighting approaches of FR and AHP.

values as shown in Figure 4. This is better as you would have better distribution of values in each classes than the commonly used natural breaks where some classes might have a limited or excessive number of values.

4.2. Object-based

Weights from the data-driven FR and expert-based AHP approaches were used for the aggregation based on the object-based geon. The weights were used for segmentation to produce the landslide susceptibility maps based on geon. The resulting Landslide Susceptibility maps for each weighting approach are shown in Figure 5. The resulting values in the maps were classified based on the same quantile classification method as described above.

It is essential to understand how the final landslide susceptibility maps were derived through each model and how each conditioning factor influences them. The final weightings influence the resulting map, but it is unclear how each location is affected by each conditioning factor. To demonstrate the impact of the conditioning factors, we chose four random locations in the resulting map derived using the geon approach (two locations for FR and two locations for AHP) and assessed the impact of each conditioning factor in these four random locations.

Figure 6 shows the two locations chosen for the geon where the weights are derived from FR.

Figure 7 shows the impact of the conditioning factors for location one (see Figure 6). It indicates that the distance to drainage has the highest influence, followed by lithology and geology. The distance to roads has the least impact at this location. Location one in the final susceptibility map is categorized as a high susceptibility area.

At location two (see Figure 6), geology has the most significant impact while distance to drainage, rainfall, distance to faults and elevation have the least impact on the final susceptibility map. Location two has been categorized as a very low susceptibility area. The effect of each conditioning factor at location two can be seen in Figure 8.

Location one in Figure 9, where the weights for the geon are derived from AHP has been categorized as a very high susceptible area in the final susceptibility map. The most significant impact is from rainfall followed by lithology and geology, whereas the least impact is from distance to roads followed by elevation. The impact of each conditioning factor for location one is shown in Figure 10.

Location two in Figure 9, where the weights for the geon are derived from AHP, has been categorized as being moderately susceptible in the final susceptibility map. The most significant maximum impact is from geology and distance to drainage, whereas the least impact is from elevation. The impact of each conditioning factor for location two is shown in Figure 11

The geon model has an advantage over other models because it shows the impact of each conditioning factor on the final landslide susceptibility map for homogenous units instead of for single grids, which can help to better understand and interpret the results. The results of the grid-based approach, on the other hand, are more complex to show and communicate, which makes the geon a meaningful unit.

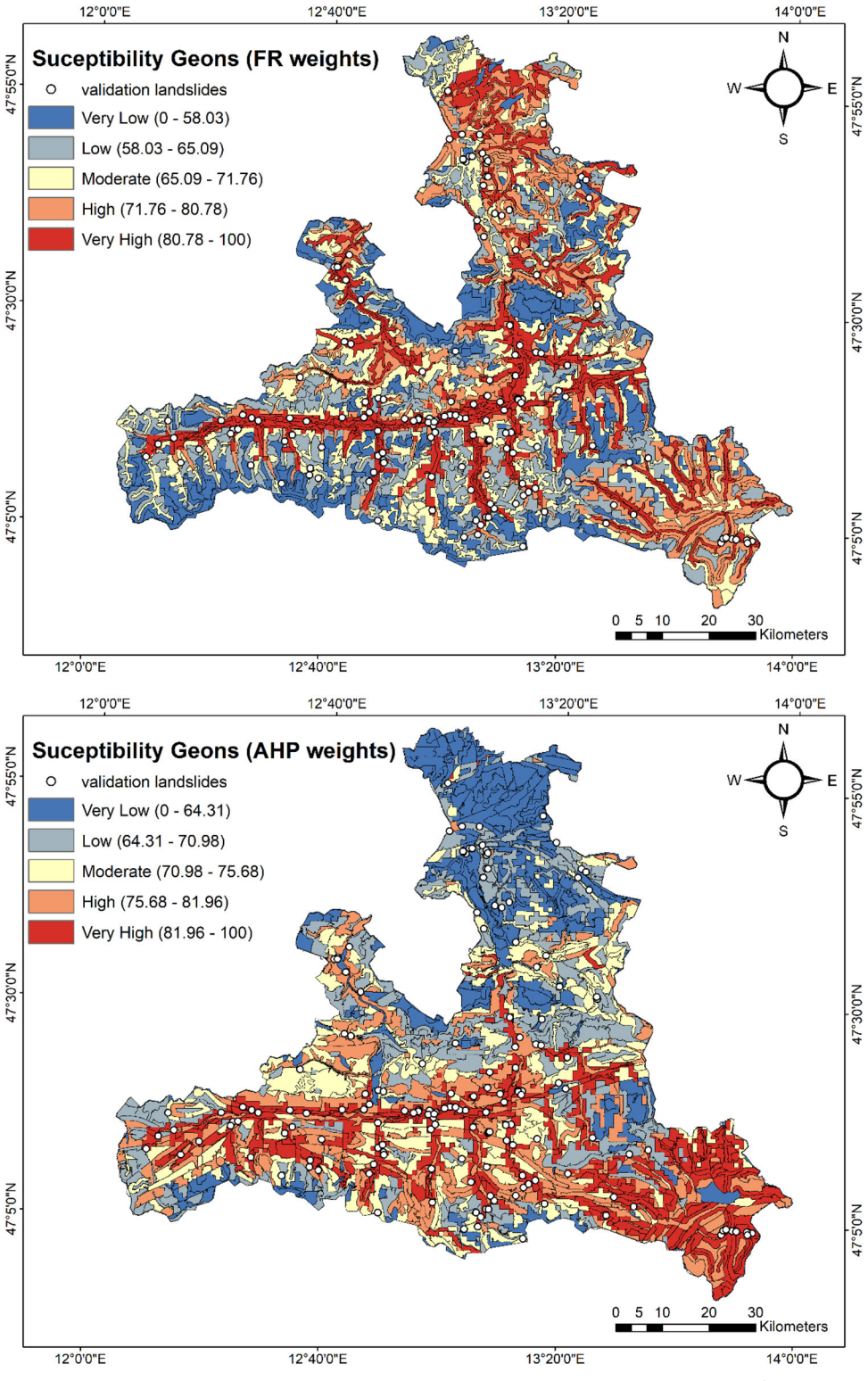

Figure 5. Landslide susceptibility maps derived using the object-based approach of geon using weights from FR and AHP.

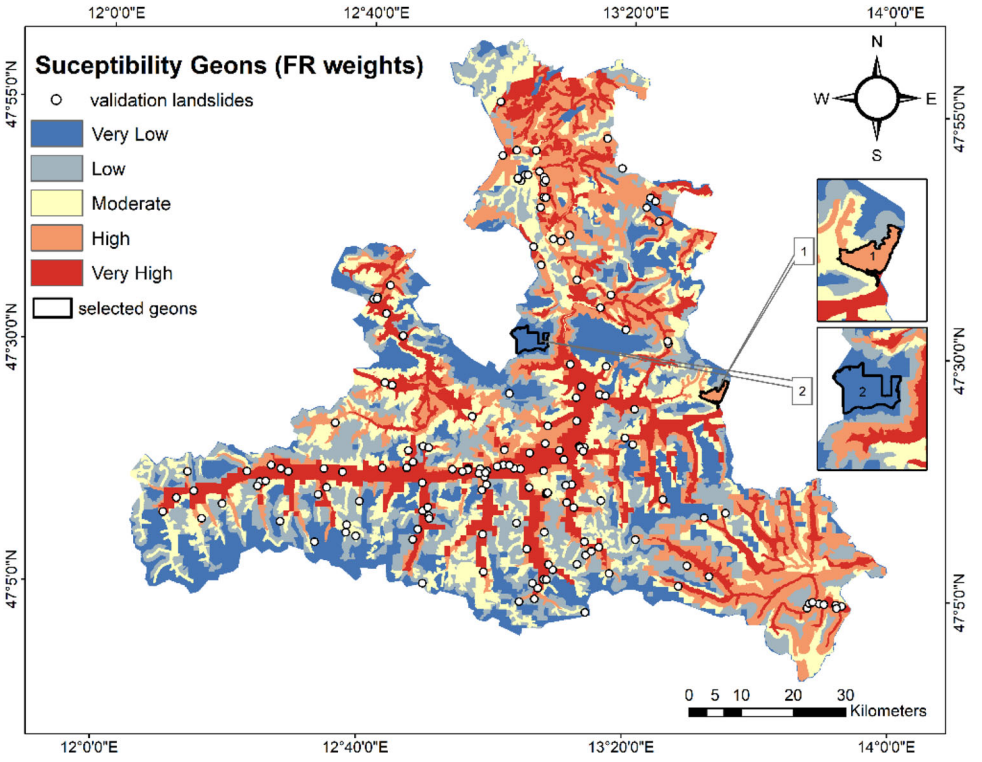

Figure 6. Selected geon for the impact assessment of each conditioning factor on the final susceptibility map using the geon approach based on FR weights.

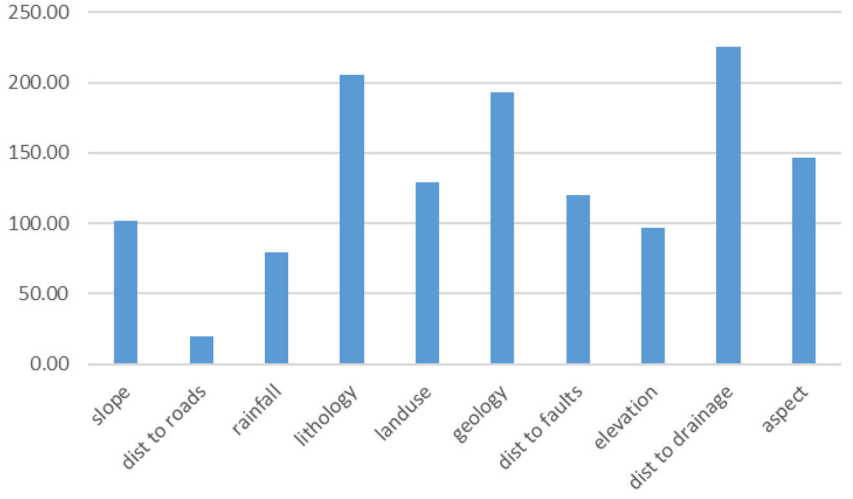

Figure 7. Impact of each conditioning factor at location one based on the geon approach using FR weights.

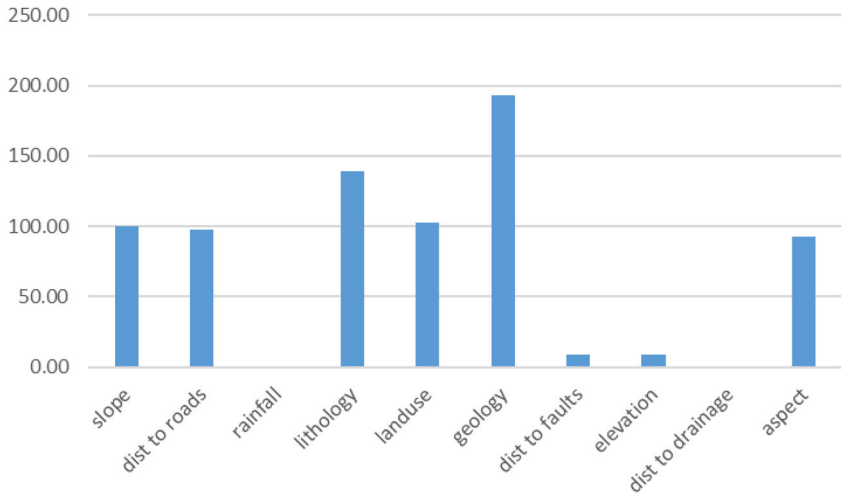

Figure 8. Impact of each conditioning factor at location two based on the geon approach using FR weights.

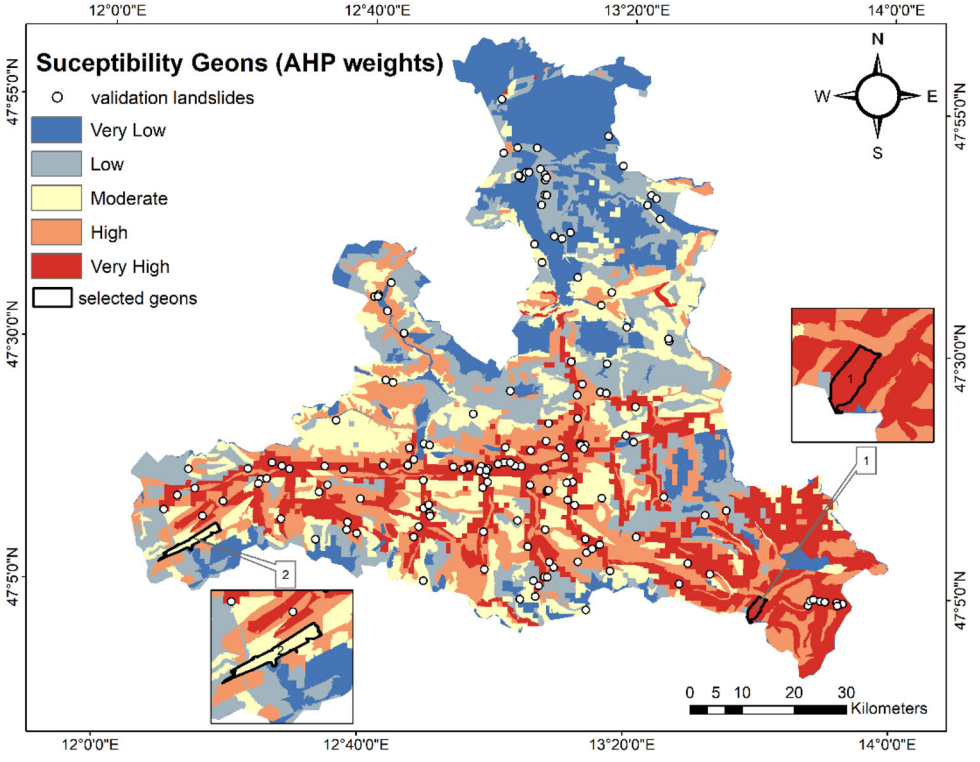

Figure 9. Selected geon for the impact assessment of each conditioning factor on the final susceptibility map using the geon approach based on AHP weights.

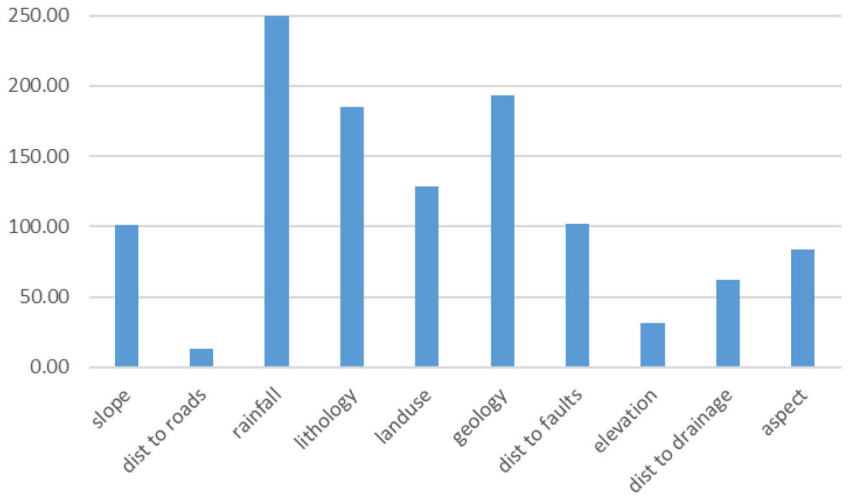

Figure 10. Impact of each conditioning factor in location 1 based on the geon approach using AHP weights.

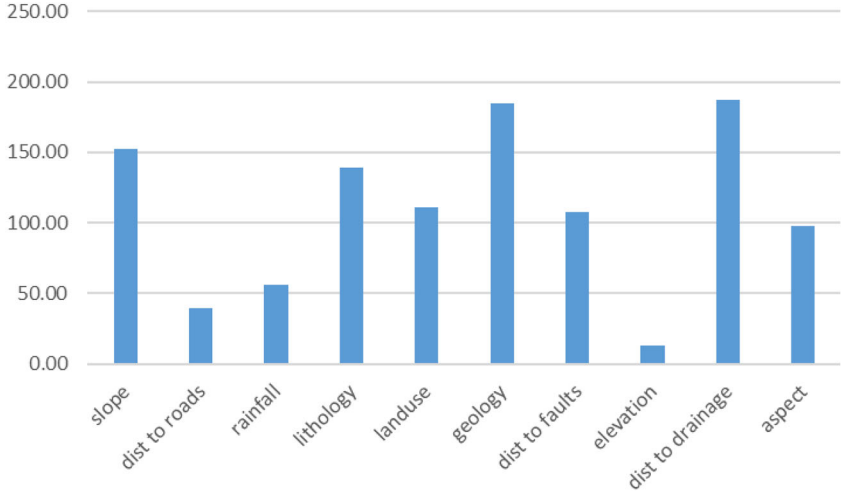

Figure 11. Impact of each conditioning factor at location two based on the geon approach using AHP weights.

5. Validation

Validation is an integral part of landslide susceptibility mapping (Ghorbanzadeh et al. 2018a), in particular, to produce information which is of practical benefit for decision-makers. To determine the success of the applied landslide susceptibility models, we compared the resulting maps from each of the models with the existing landslide inventory data. To get an indication of the effectiveness of each model for LSM, analysis of the conformity between the inventory data and the resulting maps indicates whether the applied models can correctly predict the areas that are susceptible to landslides (Pourghasemi and Rahmati 2018). 30% of the point locations from the landslide inventory (i.e. 167 landslides) were used as reference data for validating the results.

5.1. Receiver Operating Characteristics (ROC)

The receiver operating characteristics (ROC) curve was used to validate the four resulting landslide susceptibility maps made using the FR, AHP, geon AHP and geon FR using the validation data. The ROC approach enables a comparison of the true positive rate (TPR) and the false positive rate (FPR) in the landslide susceptibility maps (Linden 2006; Ghorbanzadeh et al. 2018d). ROC curves were calculated for all landslide susceptibility maps. Pixels that are correctly identified (high susceptibility) and thus match the landslide reference data are the TPRs, while the incorrectly labelled pixels are the FPRs. ROC curves are generated by plotting the TPRs versus FPRs. The area under the curve (AUC) is the degree that specifies the accuracy of the resulting landslide susceptibility maps. The AUC indicates the probability that more pixels were correctly labelled than incorrectly labelled. Greater AUC values indicate a higher accuracy and lower AUC values indicate lower accuracy of the susceptibility map. If the AUC values are close to unity, then this indicates a significant susceptibility map. A value of 0.5 shows an insignificant map because it means the map was generated by coincidence (Baird et al. 2013).

The AUC values obtained from the ROC approach for FR, AHP, Geon (FR) and Geon (AHP) were 0.89. 0.88, 0.90 and 0.89, respectively. According to the results, the geon approach indicates more accurate results compared to the per-pixel based FR and AHP. The results of AHP may vary as this method is based on the expert weightings and thus on the knowledge of the experts. Figure 12 represents the ROC quality method success rate curves for FR, AHP, Geon (FR) and Geon (AHP) using the validation landslide inventory data, and Figure 13 represents the ROC quality method success rate curves for FR, AHP, Geon (FR) and Geon (AHP) using the training landslide inventory data.

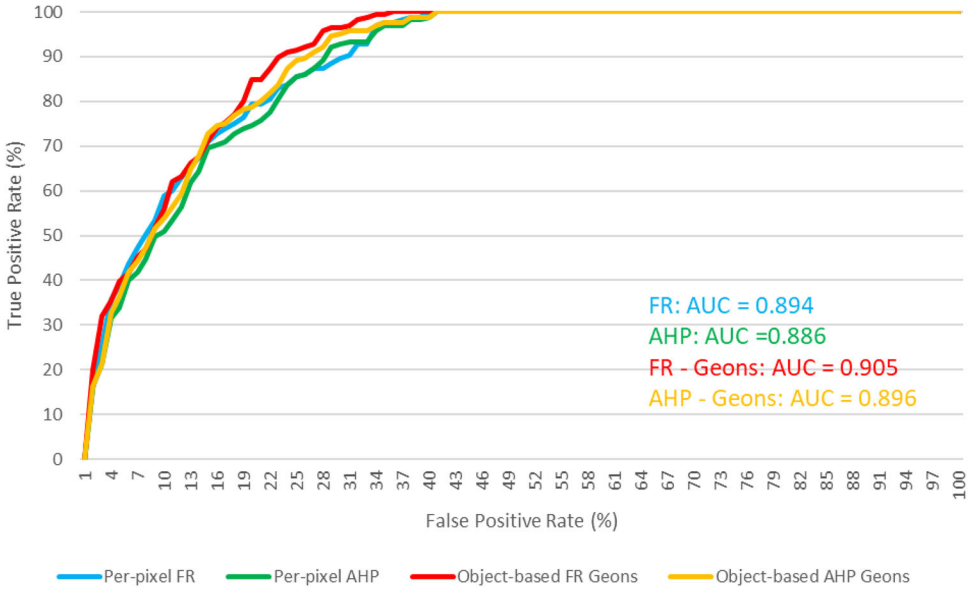

Figure 12. The ROC representing the quality method success rate curves for the FR, AHP, geon (FR), and geon (AHP) approaches using the validation landslide data.

5.2. Relative Landslide Density (R-index)

Additionally, the accuracy of the resulting LSMs was evaluated using the index of relative landslide density (R-index). The R-index can be calculated using Equation (4):

$$R = (ni/Ni)/\Sigma(ni/Ni)) \times 100 \quad (4)$$

where Ni is the percentage of landslides in each susceptibility class, and ni is the percentage of the area that is susceptible to landslides in each susceptibility class. Table 4 shows the four approaches categorized into five susceptibility classes using the

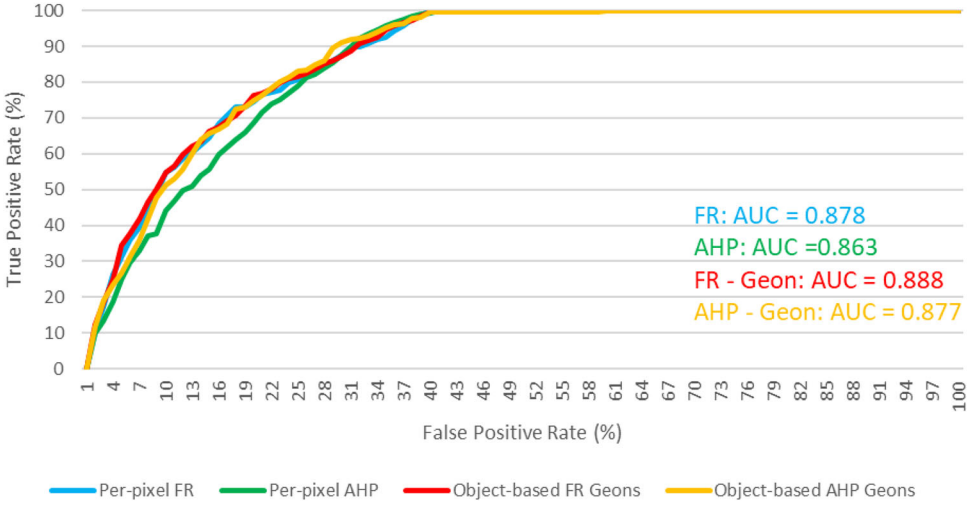

Figure 13. The ROC representing the quality method success rate curves for the FR, AHP, geon (FR), and geon (AHP) approaches using the training landslide data.

Table 4. R-indexes for the landslide susceptibility mappings (LSMs) of FR, AHP, Geon (FR) and Geon (AHP).

Validation methods	Susceptibility class	Number of pixels	Area (km^2)	Area (%) (ni)	Number of landslides	Landslide (%) (Ni)	R-index
AHP	Very Low	7200	2069.52	29.10	9	5.39	2
	Low	29700	2259.21	31.77	33	19.76	7
	Moderate	41400	1640.52	23.07	47	28.14	14
	High	43200	8424.08	11.85	48	28.74	28
	Very high	27000	3001.68	4.22	30	17.96	49
FR	Very Low	9900	1422.69	20.00	11	6.59	7
	Low	9900	1422.32	20.00	12	7.19	7
	Moderate	13500	1422.29	20.00	15	8.98	9
	High	32400	1422.56	20.00	37	22.16	22
	Very high	82800	1421.94	19.99	92	55.09	55
Geon (FR)	Very Low	8100	1443.69	20.10	9	5.39	5
	Low	12600	1435.06	19.98	12	7.19	7
	Moderate	16200	1435.68	19.99	16	9.58	10
	High	32400	1436.61	20.00	34	20.36	20
	Very high	81000	1430.90	19.92	96	57.49	58
	Very Low	7200	1439.59	20.03	8	4.79	5
	Low	17100	1439.79	20.03	19	11.38	11
Geon (AHP)	Moderate	21600	1441.36	20.06	24	14.37	14
	High	26100	1433.05	19.94	29	17.37	17
	Very high	78300	1432.77	19.94	87	52.10	53

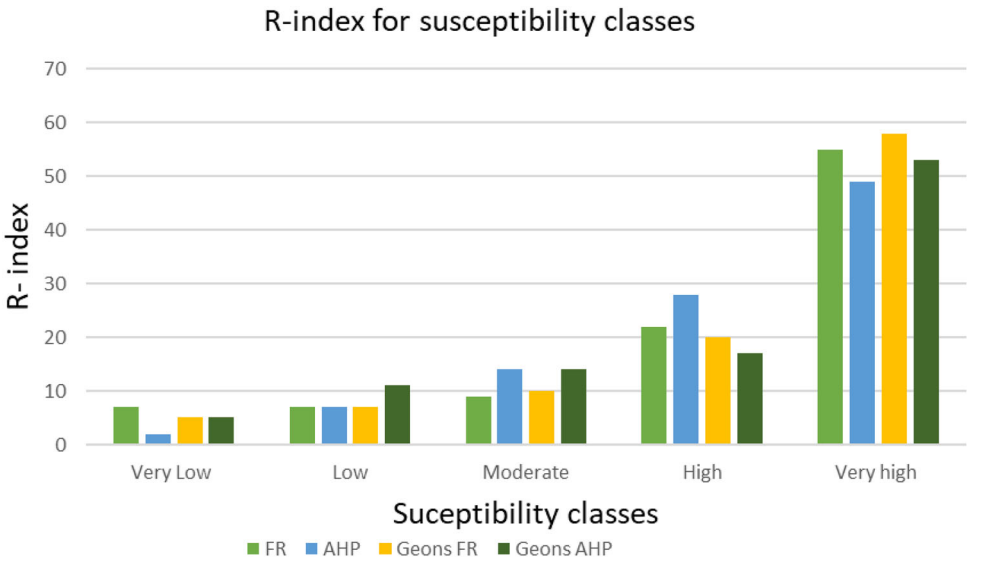

Figure 14. Results of R-index plots for AHP, FR and geon.

quantile classification method. Overall, the geon-based aggregation method shows a higher r-index for higher susceptibility classes compared to the FR and AHP methods. The R-index results show that the Geon (FR) has higher r-index value for the very high susceptibility class compared to the AHP method, which has the lowest r-index for the very high susceptibility class. The AHP method has a higher r-index value for the high susceptible class compared to the other three approaches. The AHP method also has the lowest r-index for the very low susceptibility class. The R-index values for the high susceptibility class in AHP, FR, Geon (FR) and Geon (AHP) are 49%, 55%, 58% and 53%, respectively

The geon model achieved better results compared to the per-pixel FR and AHP models when considering the difference in the areas of the susceptibility classes and the subsequent R-index for each class.

Figure 14 shows the r-index for each susceptibility class categorized into five classes based on the quantile classification.

6. Discussion

The results reveal a range of possibilities for the use of the object-based aggregation concept of geon for landslide susceptibility mapping. The core idea of the geon approach is that the final susceptible entities are independent of administrative units. It can, therefore, reduce the biases from artificial borders in the landscape. Additionally, geons also facilitate the identification of place-specific implementation measures which are better for landslide susceptibility management that does not take into account the boundary restrictions. In general, geons allow transforming continuous spatial information into discrete objects in order to monitor changes according to various hazards in a specific area. This study may support spatial planners in decision-making and presents a strategic and regionalised susceptibility mapping method that determines homogeneous

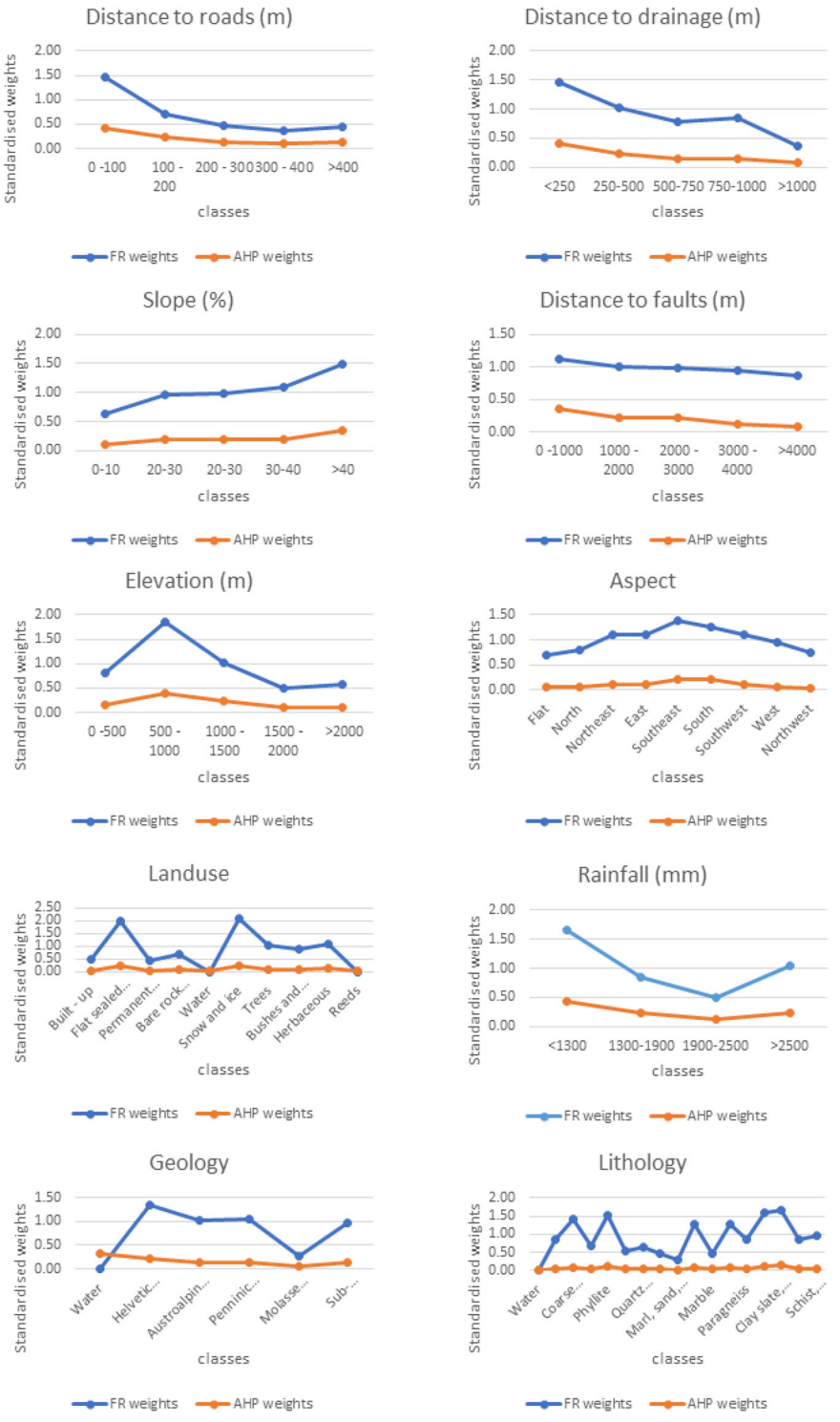

Figure 15. Comparison of the resulting weights for each factor and the classes based on the FR and AHP model.

landscape units and does not adhere to administrative boundaries. The advantage of using the geons model is that it allows us to understand the impact of each conditioning factor used in the study area on the final susceptibility map. A proper understanding of the impact of the conditioning factors in each location is crucial for understanding the mechanism of landslide occurrences at a regional scale.

Geology is one of the most significant factors that affect landslides. It can be interpreted from Table 2 that among the weights derived from FR and AHP approaches for all the conditioning factors, geology is one of the most influencing factors derived from the landslide inventory in Salzburg. In the impact study of each conditioning factor in Figure 7 to Figure 11, geology plays an important role and has one of the highest values in the final susceptibility map in the four chosen location and influences the susceptibility classes. The geological conditions highly influence the occurrence of landslides along with the influence of human activities.

While the data-driven FR approach is a simple and easy to apply method, the multi-criteria based AHP is more complex and requires domain knowledge and expert judgement to assign weights to each conditioning factor. The FR approach permits the evaluation of relationships between a dependent variable and several independent variables in a discrete form. By contrast, the AHP allows evaluating the continuous independent variables in addition to distinct forms (Schicker and Moon 2012).

The overall results obtained from the ROC approach show that the geon (FR) model yielded a higher accuracy, followed by the FR model. The AHP model yielded the lowest accuracy compared to the geon and the FR model. The higher accuracy of the FR model compared to the AHP model shows that the data-driven methodology performs better than the expert-based AHP method, at least in the present study. However, the results might vary depending on the experts and the knowledge domain for assigning the criteria weights in that particular region. Many researchers combine the AHP method with other methodologies such as Dempster Shafer or fuzzy theory to improve the final landslide susceptibility maps. We used the conventional FR and AHP methods, as we wanted to compare the two traditional per-pixel weighting methods of FR and AHP with the object-based aggregation methodology of the geon approach. The resulting susceptibility map is based on the landslide point inventory, and the results might vary when using other polygon-based landslide inventories.

As presented in Figure 15, most of the weightings of the sub-criteria based on the AHP and FR models are different in absolute terms but show similarities in some classes. According to the results based on the AHP, for example, the elevation class of 500-1000 m is the most important in terms of landslide susceptibility with a weighting of 0.39. Similarly, based on the weighting of the FR model, the class of 500-1000 m is the most significant class with a weighting of 1.86. The weightings of the AHP and FR models for the criteria distance to roads and distance to drainage follow a very similar pattern but also show different weightings.

7. Conclusions

Landslide susceptibility mapping is for assessing landslide-prone areas. The results can help to better manage and plan risk mitigation measures. So far, no detailed

landslide susceptibility analysis has been carried out for the Province of Salzburg. In this study, we produced landslide susceptibility maps for the entire Province of Salzburg using FR, AHP and the geon method and compared a per-pixel weighting approach with an object-based aggregation approach. We used 560 landslide locations, of which 70% were used for training and 30% for validation. The accuracy and the degree of fit of the resulting landslide susceptibility maps were validated using two approaches, namely the ROC and R-index. The results of this validation show that all four methods can be applied for landslide susceptibility mapping, leading to similar AUC values: FR (0.89), AHP (0.88), Geon (FR) (0.90) and Geon (AHP) (0.89). However, the object-based geon model showed slightly higher accuracy results. The validation results demonstrate that object-based models are suited for landslide susceptibility and can even lead to higher accuracies compared to the pixel-based FR and AHP approaches. Geon represents meaningful units, and thus, are likely more suitable than per-pixel approaches for planning and mitigation.

We used a point-based landslide inventory for this study. A complementary study could employ a polygon-based landslide inventory dataset to check and compare the accuracy of the methodology and the effect of the input data. For future work, the geon approach could be compared with machine learning approaches and deep learning approaches.

This research introduces the use of geon as an object-based aggregation approach for landslide susceptibility mapping. This method may also be applied to analyze the susceptibility of other hazards. The resulting susceptibility maps can be useful for local administration and civil protection entities in cases of further events or continuous motion of landslides to evaluate potentially affected areas. This study illustrates that geon can be used to obtain meaningful susceptibility regions. The respective results can be beneficial for planners and disaster management to identify the regions prone to landslides and to mitigate the financial and economic damage from landslides in future.

Acknowledgements

Authors like to thank the Geological Survey of Austria (GBA) for providing the Landslide inventory data. We also would like to thank autonomous reviewers for their constructive inputs on the manuscript.

Funding

This research was partially funded by the Austrian Science Fund FWF through the GIScience Doctoral College (DK W 1237-N23) at the University of Salzburg. D. Hölbling has been supported by the Austrian Academy of Sciences (ÖAW) through the project RiCoLa (Detection and analysis of landslide-induced river course changes and lake formation).

ORCID

Thimmaiah Gudiyangada Nachappa http://orcid.org/0000-0002-1341-3264
Stefan Kienberger http://orcid.org/0000-0002-4800-4516

Sansar Raj Meena http://orcid.org/0000-0001-6175-6491
Daniel Hölbling http://orcid.org/0000-0001-9282-8072
Thomas Blaschke http://orcid.org/0000-0002-1860-8458

References

Baatz M, Schäpe A. 2000. Multi resolution segmentation: an optimum approach for high quality multi scale image segmentation. In: Beutrage zum AGIT-Symposium. Salzburg, Heidelberg, 2000. p. 12–23

Baird C, Healy T, Johnson K, Bogie A, Dankert EW, Scharenbroch C. 2013. A comparison of risk assessment instruments in juvenile justice. Madison, (WI): National Council on Crime and Delinquency

Bartelletti C, Giannecchini R, D'Amato Avanzi G, Galanti Y, Mazzali A. 2017. The influence of geological–morphological and land use settings on shallow landslides in the Pogliaschina T. basin (northern Apennines, Italy). J Maps. 13:142–152

Blaschke T. 2010. Object based image analysis for remote sensing ISPRS. J Photogramm Remote Sens. 65:2–16

Cabrera-Barona P, Ghorbanzadeh O. 2018. Comparing classic and interval analytical hierarchy process methodologies for measuring area-level deprivation to analyze health inequalities. Int J Environ Res Public Health. 15:140

Casagli, N, Cigna, F, Bianchini, S, Holbling, D, Fureder, P, Righini, G, Del Conte, S, Friedl, B, Schneiderbauer, S, Iasio, C. et al. 2016. Landslide mapping and monitoring by using radar and optical remote sensing: Examples from the EC-FP7 project SAFER. RSA: Soc Envir. 4: 92–108

Chen W, Pourghasemi HR, Naghibi SA. 2017. A comparative study of landslide susceptibility maps produced using support vector machine with different kernel functions and entropy data mining models in China. B Eng Geol Environ. 77:647–664

Demir G, Aytekin M, Akgün A, İkizler SB, Tatar O. 2012. A comparison of landslide susceptibility mapping of the eastern part of the North Anatolian Fault Zone (Turkey) by likelihood-frequency ratio and analytic hierarchy process methods. Nat Hazards. 65:1481–1506

Dragut L, Csillik O, Eisank C, Tiede D. 2014. Automated parameterisation for multi-scale image segmentation on multiple layers ISPRS J Photogramm Remote Sens. 88:119–127

Drăguţ L, Tiede D, Levick SR. 2010. ESP: a tool to estimate scale parameter for multiresolution image segmentation of remotely sensed data. Int J Geogr Inf Sci. 24:859–871

Feizizadeh B, Blaschke T. 2014. An uncertainty and sensitivity analysis approach for GIS-based multicriteria landslide susceptibility mapping. Int J Geogr Inf Sci. 28:610–638

Ghorbanzadeh O, Blaschke T, Aryal J, Gholaminia K. 2018a. A new GIS-based technique using an adaptive neuro-fuzzy inference system for land subsidence susceptibility mapping. J Spat Sci. 94:1–17

Ghorbanzadeh O, Feizizadeh B, Blaschke T. 2017. Multi-criteria risk evaluation by integrating an analytical network process approach into GIS-based sensitivity and uncertainty analyses. Geomat Nat Haz Risk. 9:127–151

Ghorbanzadeh O, Feizizadeh B, Blaschke T, Khosravi R. 2018b. Spatially explicit sensitivity and uncertainty analysis for the landslide risk assessment of the gas pipeline networks. Paper presented at: The 21st AGILE conference on Geo-information science., Lund, Sweden,

Ghorbanzadeh O, Moslem S, Blaschke T, Duleba S. 2018c. Sustainable urban transport planning considering different stakeholder groups by an interval-AHP decision support model. Sustainability. 11:1–18

Ghorbanzadeh O, Rostamzadeh H, Blaschke T, Gholaminia K, Aryal J. 2018d. A new GIS-based data mining technique using an adaptive neuro-fuzzy inference system (ANFIS) and k-fold cross-validation approach for land subsidence susceptibility mapping. Nat Hazards. 94:497–517

Glade T, Petschko H, Bell R, Bauer C, Granica K, Heiss G, Leopold P, Pomaroli G, Proske H, Schweigl J. 2012. Landslide susceptibility maps for Lower Austria–Methods and Challenges. Koboltschnig, G., Hübl, J., Braun, J, editors. International Research Society INTERPRAEVENT, vol. 1 Grenoble, France: p. 497–508

Gordo C, Zêzere JL, Marques R. 2019. Landslide susceptibility assessment at the basin scale for rainfall- and earthquake-triggered shallow slides. Geosciences 9:1–22

Guzzetti F, Mondini AC, Cardinali M, Fiorucci F, Santangelo M, Chang K-T. 2012. Landslide inventory maps: New tools for an old problem. Earth-Sci Rev. 112:42–66

Hagenlocher M, Kienberger S, Lang S, Blaschke T. 2014. Implications of spatial scales and reporting units for the spatial modelling of vulnerability to vector-borne diseases GI_Forum 2014:197

Haque U, Blum P, da Silva P F, Andersen P, Pilz J, Chalov SR, Malet J-P, Auflič MJ, Andres N, Poyiadji E. et al. 2016. Fatal landslides in Europe. Landslides. 13:1545–1554

Höller P. 2009. Avalanche cycles in Austria: an analysis of the major events in the last 50 years. Nat Hazards. 48:399–424

Hong H, Pradhan B, Xu C, Tien Bui D. 2015. Spatial prediction of landslide hazard at the Yihuang area (China) using two-class kernel logistic regression, alternating decision tree and support vector machines. Catena. 133:266–281

Kayastha P, Dhital MR, De Smedt F. 2013. Application of the analytical hierarchy process (AHP) for landslide susceptibility mapping: a case study from the Tinau watershed, west Nepal. Comput Geosci. 52:398–408

Kienberger S, Lang S, Zeil P. 2009. Spatial vulnerability units - expert-based spatial modelling of socio-economic vulnerability in the Salzach catchment, Austria. Nat Hazards Earth Syst Sci. 9:767–778

Lang S, Kienberger S, Tiede D, Hagenlocher M, Pernkopf L. 2014. Geons – domain-specific regionalization of space. Cartography Geo Inf Sci. 41:214–226

Lee S, Pradhan B. 2006. Landslide hazard mapping at Selangor, Malaysia using frequency ratio and logistic regression models. Landslides. 4:33–41

Li R, Wang N. 2019. Landslide susceptibility mapping for the muchuan county (China): a comparison between bivariate statistical models (WoE, EBF, and IoE) and their ensembles with logistic regression. Symmetry. 11:762

Lima P, Steger S, Glade T, Tilch N, Schwarz L, Kociu A (2017) Landslide susceptibility mapping at national scale: a first attempt for Austria. In: Mikos M, Tiwari B, Yin Y, Sassa K, editors. Advancing Culture of Living with Landslides. , Advances in Landslide Science. Volume 2. Springer, Cham, 2017, 943–951.

Linden A. 2006. Measuring diagnostic and predictive accuracy in disease management: an introduction to receiver operating characteristic (ROC) analysis. J Eval Clin Pract. 12: 132–139

Mahalingam R, Olsen MJ, O'Banion MS. 2016. Evaluation of landslide susceptibility mapping techniques using lidar-derived conditioning factors (Oregon case study) Geomatics, Nat Haz Risk. 7:1884–1907

Malczewski J. 1999. GIS and multicriteria decision analysis. :John Wiley & Sons, New York

Malczewski J. 2006. GIS-based multicriteria decision analysis: a survey of the literature. Int J Geogr Inf Sci. 20:703–726

Meena S, Ghorbanzadeh O, Blaschke T. 2019a. A Comparative study of statistics-based landslide susceptibility models: a case study of the region affected by the Gorkha earthquake in Nepal. ISPRS Int. J. Geo-Inf. 8: 1–23.

Meena S, Mishra B, Tavakkoli Piralilou S. 2019b. A hybrid spatial multi-criteria evaluation method for mapping landslide susceptible areas in Kullu Valley, Himalayas. Geosciences. 9: 1–18

Persichillo MG, Bordoni M, Meisina C. 2017. The role of land use changes in the distribution of shallow landslides. Sci Total Environ. 574:924–937

Petschko H, Brenning A, Bell R, Goetz J, Glade T. 2014. Assessing the quality of landslide susceptibility maps–case study Lower Austria Nat Hazards Earth Syst Sci. 14:95–118

Pham BT, Indra P, Khosravi K, Chapi K, Trinh PT. Ngo TQ, Hosseini SV, Bui DT. 2018. A comparison of Support Vector Machines and Bayesian algorithms for landslide susceptibility modelling. Geocarto Int. 34:1385–1407

Pirnazar M, Karimi A, Feizizadeh B, Ostad-Ali-Askari K, Eslamian S, Hasheminasab H, Ghorbanzadeh O, Hamedani M. 2017. Assessing flood hazard using gis based multi-criteria decision making approach; study area: east-azerbaijan province (Kaleybar Chay basin). J flood engr. 8: 203–223

Pourghasemi HR, Rahmati O. 2018. Prediction of the landslide susceptibility: Which algorithm, which precision?. Catena. 162:177–192

Raja NB, Çiçek I, Türkoğlu N, Aydin O, Kawasaki A. 2017. Correction to: landslide susceptibility mapping of the sera river Basin using logistic regression model. Nat Hazards. 91: 1423–1423

Roodposhti MS, Aryal J, Pradhan B. 2019. A Novel Rule-based Approach In Mapping Landslide Susceptibility.Sensors (Basel). 19(10), 2274.

Saaty TL. 1980. The analytic process: planning, priority setting, resources allocation New York: McGraw

Saaty TL, Vargas LG. 1984. Inconsistency and rank preservation. J Math Psychol. 28:205–214

Saaty TL, Vargas LG. 1991. Prediction, projection, and forecasting: applications of the analytic hierarchy process in economics, finance, politics, games, and sports. :Kluwer Academic Pub.

Sahnoun H, Serbaji MM, Karray B, Medhioub K. 2011. GIS and multi-criteria analysis to select potential sites of agro-industrial complex. Envi Earth Sci. 66:2477–2489

Scaioni M, Longoni L, Melillo V, Papini M. 2014. Remote sensing for landslide investigations: an overview of recent achievements and perspectives. Remote Sens. 6:9600–9652

Schicker R, Moon V. 2012. Comparison of bivariate and multivariate statistical approaches in landslide susceptibility mapping at a regional scale. Geomorphology. 161-162:40–57

Sestraș P, Bilașco Ș, Roșca S, Naș S, Bondrea MV, Gâlgău R, Vereș I, Sălăgean T, Spalević V, Cîmpeanu SM. 2019. Landslides Susceptibility Assessment Based on GIS Statistical Bivariate Analysis in the Hills Surrounding a Metropolitan Area. Sustainability. 11:

Taha R, Dietrich J, Dehnhardt A, Hirschfeld J. 2019. Scaling effects in spatial multi-criteria decision aggregation in integrated river Basin management. Water 11, 355.

Tay LT, Lateh H, Hossain K, KamilAA. 2014. Landslide Hazard Mapping of Penang Island Using Poisson Distribution with Dominant Factors. J Civ Eng Res. 4(3A): 72–77

Tiede D, Lang S, Albrecht F, Holbling D. 2010. Object-based class modeling for cadastre-constrained delineation of geo-objects. Photogramm Eng Rem S. 76:193–202

Tien Bui D, Khosravi K, Shahabi H, Daggupati P, Adamowski JF, Melesse AM, Pham BT, Pourghasemi HR, Mahmoudi M, Bahrami S. et al. 2019. Flood spatial modeling in Northern Iran using remote sensing and GIS: a comparison between evidential belief functions and its ensemble with a multivariate logistic regression model. Remote Sens. 11

Tsangaratos P, Ilia I. 2016. Comparison of a logistic regression and Naïve Bayes classifier in landslide susceptibility assessments: The influence of models complexity and training dataset size. Catena 145:164–179

Umar Z, Pradhan B, Ahmad A, Jebur MN, Tehrany MS. 2014. Earthquake induced landslide susceptibility mapping using an integrated ensemble frequency ratio and logistic regression models in West Sumatera province, Indonesia. Catena. 118:124–135

Wang Q, Li W. 2017. A GIS-based comparative evaluation of analytical hierarchy process and frequency ratio models for landslide susceptibility mapping. Phys Geogr. 38:318–337

Wu Y, Li W, Wang Q, Liu Q, Yang D, Xing M, Pei Y, Yan S. 2016. Landslide susceptibility assessment using frequency ratio, statistical index and certainty factor models for the Gangu County, China. Arab. J. Geosci. 9

Yalcin A, Bulut F. 2006. Landslide susceptibility mapping using GIS and digital photogrammetric techniques: a case study from Ardesen (NE-Turkey). Nat Hazards. 41:201–226